

https://doi.org/10.1070/QEL16580

Numerical analysis of amplification of picosecond pulses in a THL-100 laser system with an increase in the pump energy of the XeF(C–A) amplifier

A.G. Yastremskii, N.G. Ivanov, V.F. Losev

Abstract. **Energy characteristics of laser radiation with a pulse width of 50 ps at an elevated pump energy of the XeF(C–A) amplifier of a hybrid THL-100 laser system are analysed numerically. The dynamics of the change in the energy and maximum intensity of laser radiation with an increase in the pump energy of the XeF(C–A) amplifier from 270 to 400 J is investigated. The results of studying the influence of the input beam divergence on the energy characteristics of the output beam are presented. It is shown that, for the existing system of mirrors, an increase in the pump energy to 400 J leads to an increase in the output energy from 3.2 to 5.5 J at a maximum radiation intensity of 57 GW cm^{-2}. A system of amplifier mirrors with 27 laser beam passes and enlarged divergence angle of the amplified beam is considered. Theoretically, the proposed system of mirrors allows one to increase the laser pulse energy to 7.5 J at a maximum intensity of no more than 14.8 GW cm^{-2}. The calculated efficiency of the conversion of the pump energy absorbed in the amplifier gas chamber into the lasing energy exceeds 3% in this regime.**

Keywords: *hybrid THL-100 laser system, amplification of picosecond pulses, laser radiation energy, numerical simulation.*

1. Introduction

Currently, terawatt and petawatt laser beams play an important role in the development of new fields of modern physics, such as acceleration of high-energy electron and ion beams with record current density, generation of attosecond pulses in the X-ray range, initiation of nuclear reactions, etc. Systems based on solid-state Ti:sapphire lasers, operating in the IR spectral region, are being intensively developed [1, 2]. However, radiation with smaller wavelengths, whose interaction efficiency with environment is much higher, is called for in many cases.

In 1979, L.D. Mikheev and colleagues showed good prospects of the C–A transition in the XeF molecule for amplifying femtosecond laser pulses in the visible spectral range (λ = 475 nm). A hybrid scheme of multiterawatt laser systems was proposed [3–8]. Based on this scheme, researchers from the Institute of High-Current Electronics, Siberian Branch of the Russian Academy of Sciences, developed (in cooperation with the Lebedev Physical Institute, Russian Academy of Sciences) a hybrid THL-100 laser system, consisting of a Ti:sapphire laser front end, a second-harmonic generator, a stretcher based on a prism pair, a photochemical XeF(C–A) amplifier, and a compressor in the form of a block of fused silica plates [9, 10].

This system can operate using two optical schemes. The first is based on amplification of a negatively chirped picosecond pulse in a gas amplifier, with its subsequent temporal compression in the glass bulk, while the second one implies amplification of a positively chirped subnanosecond pulse, with its subsequent compression in a diffraction grating compressor.

The operation of this facility using the first scheme made it possible to obtain experimentally a laser pulse power of 14 TW at a wavelength λ = 475 nm, which is a record value for the visible wavelength region [9, 10].

The results of the experiments on amplification of laser radiation with energy E_{in} = 0.8 mJ and pulse FWHM $T_{fw} \sim$ 2 ps were reported in [11]. At a VUV pump energy E_{VUV} = 260 J, the beam energy at the amplifier output was 2 J (the corresponding calculated value was 2.38 J). After upgrading the system, the maximum energy obtained within the first scheme amounted to 2.5 J, and the intensity I_{max} reached 64 GW cm^{-2} [12].

An application of the second optical scheme at $E_{VUV} \approx$ 270 J and E_{in} = 2 mJ made it possible to increase the laser output energy E_{out} at the XeF(C–A) amplifier output to 3.2 J [13–15] (the calculated value is 3.8 J) at a maximum laser beam intensity of 6.3 GW cm^{-2} (calculation). An increase in E_{in} does not lead to a rise in the output energy; hence, one can state that the XeF(C–A) amplifier operates in the saturation regime [14, 15]. A more efficient system of mirrors should be used in the XeF(C–A) amplifier in order to increase the output radiation energy even more.

This work was performed within the cycle of studies aimed at increasing the output energy for the hybrid THL-100 laser system. The purpose was to carry out a numerical analysis of the influence of the mirror system configuration in the XeF(C–A) amplifier, the pump parameters, the divergence angle (set artificially), and the energy of input radiation with a pulse width of 50 ps on the energy characteristics of output radiation.

2. Numerical model and calculation technique

The THL-100 laser system was described in detail in [9, 11–13]. A schematic of the laser-cell cross section for the XeF(C–A) amplifier and the output block of mirrors is shown in Fig. 1

A.G. Yastremskii, N.G. Ivanov Institute of High-Current Electronics, Siberian Branch, Russian Academy of Sciences, prosp. Akademicheskii 2/3, 634055 Tomsk, Russia; e-mail: yastrems@lgl.hcei.tsc.ru;
V.F. Losev Institute of High-Current Electronics, Siberian Branch, Russian Academy of Sciences, prosp. Akademicheskii 2/3, Tomsk, 634055 Russia; National Research Tomsk Polytechnic University, prosp. Lenina 30, 634050 Tomsk, Russia

Received 24 November 2017; revision received 26 December 2017
Kvantovaya Elektronika **48** (3) 206–211 (2018)
Translated by Yu.P. Sin'kov

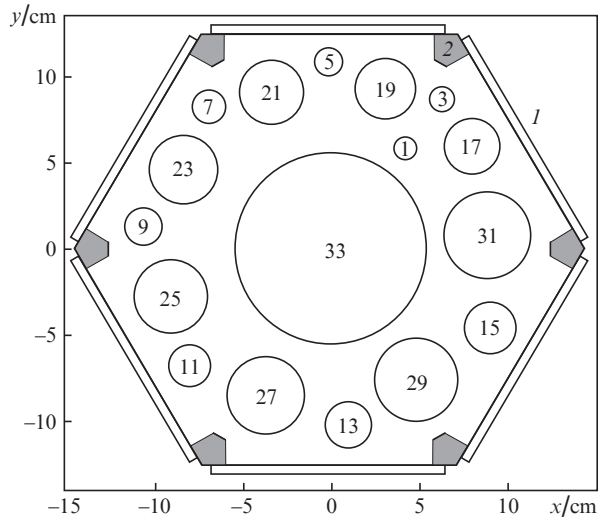

Figure 1. Scheme A of mirror arrangement in the output amplifier cascade: (*1*) input windows for VUV pumping and (*2*) regions opaque for pump radiation.

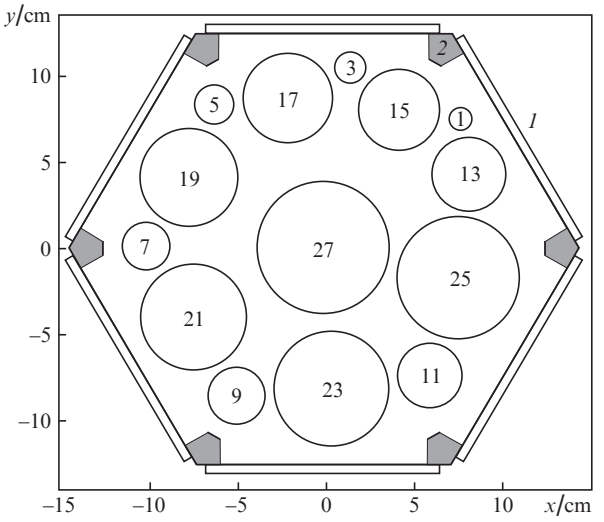

Figure 2. Scheme B of mirror arrangement in the output amplifier cascade. The designations are the same as in Fig. 1.

(we denote it as 'A'). The circle diameters are proportional to the mirror sizes; the number inside a circle is the mirror number, which is equal to the number of laser beam passes through the active medium to this mirror.

The laser beam was introduced into the cell through window 0 (omitted in Fig. 1) and extracted (after 33 passes in the active region) from the amplifier through output window 33. During the motion of the laser beam in the amplifier, its diameter increased from $D_0 = 1$ cm at the input window to $D_{31} = 5$ cm at mirror 31. The laser beam divergence angle $\Omega_{A1} = 0.95$ mrad [13] was retained constant up to convex mirror 31, at which it was increased to $\Omega_{A2} = 22$ mrad. The beam diameter at the output window was 11 cm.

The amplification regimes in which the energy maximally increases at a minimum increase in the laser beam intensity are most interesting. The rate of rise in I_{max} under amplification may be reduced when the divergence angle Ω of input laser beam increases. However, with transverse amplifier size kept invariable, an increase in angle Ω reduces the number N of laser beam passes in the amplifier active medium.

We performed a numerical analysis to find out how the number N of passes in the amplifier affects the output laser energy. The N value was varied from 25 to 39. The simulation results showed that, in the gain saturation regime, the maximum energy at a lower maximum intensity of output radiation is implemented in a system of mirrors with 27 passes in the active medium. The mirror system used in these calculations is shown in Fig. 2; it is denoted as 'B'. The input radiation divergence angle Ω_B was equal to 1.78 mrad in this case; the diameters D of the input and output windows were, respectively, 1 and 7.7 cm.

The kinetics of reactions in a N_2–XeF_2 gas mixture under VUV pumping was described in detail in [7, 16]. An active medium is formed in the amplifier upon interaction of VUV pump radiation ($\lambda = 172$ nm [9]) with XeF_2 molecules. Photolysis leads to the formation of vibrationally excited XeF(B,C) molecules, which relax, as a result of the VV and VT processes, to the ground vibrational states $XeF(B_0,C_0)$. XeF(B,C) molecules are described within this model by sets of four effective levels: XeF(B,C) (vibrational excited levels) and $XeF(B_0,C_0)$ (ground vibrational levels) for states B and C, respectively.

The model for calculating the spatiotemporal distributions of the particle concentration and UV pump radiation intensity in the amplifier gas medium was described in detail in [9, 13], where the values of necessary constants were also reported. The system of equations describing the propagation of pump radiation in the amplifier gas medium was solved in the Cartesian coordinate system X, Y, Z, using uniform rectangular computational grids. The FWHM for input radiation pulses was assumed to be $T_{fw} = 50$ ps, a value much shorter than the effective lifetime of XeF(B,C) molecules. Due to this circumstance, the computation was performed in two stages. In the first stage, the spatiotemporal distributions of gain and plasma particle concentrations were calculated. The calculation results were remembered with a time step of 1 ns. In the second stage, the laser beam gain in the amplifier was modelled. Calculations were carried out in a cylindrical coordinate system α, r, z_{las} (α and r are, respectively, the azimuthal angle and the distance from the longitudinal laser beam axis and z_{las} is the distance passed by the laser beam in the amplifier). The point with coordinates $z_{las} = 0$, $r = 0$ is located at the centre of the input window. The z_{las} axis successively passes through the mirror centres (from mirror 1 to the output window). The laser beam was introduced into the amplifier at the instant $t = t_{in}$, counted from the amplifier pumping onset.

The laser beam propagation time in the amplifier will be denoted as t_{las}. At $t_{las} = 0$, the beam leading part enters the amplifier. With an increase in the distance passed by the beam in the amplifier, its radius $R(z_{las})$ increased in correspondence with the divergence angle Ω. The dependence of the input beam fluence F_{in} on r and t_{las} is given by the Gauss formula:

$$F_{in}(\alpha, r, t_{las}) = F_{peak} \exp\left(-2\frac{r^2}{R_0^2}\right) \exp\left[-\frac{(t_{las} - t_{peak})^2}{T_{fw}^2} 4\ln 2\right]. \quad (1)$$

Here, t_{peak} is the time corresponding to maximum fluence; R_0 is the radius of the input laser beam at a level of $1/e^2$; and F_{peak} is the maximum laser beam fluence, normalised to energy E_{in}.

While the laser beam passed through the amplifier, the previously calculated spatial distribution of the concentration $n_{C_0}(x,y,t)$ of $XeF(C_0)$ molecules was recorded at the instant of beam penetration into the active region and at the instant of its emergence from this region. Then the unperturbed (i.e., in the absence of interaction between the laser radiation and active medium) distributions $n_{C_0}(\alpha,r,t_{las})$ in the laser beam cross section at these instants were calculated by the two-dimensional interpolation method [17]. The concentration $n_{C_0}(\alpha,r,t_{las})$ at intermediate points was found by linear interpolation.

The spatial distributions of the laser beam fluence $F(\alpha,r,z_{las},t_{las})$ and the concentration $n_{C_0}(\alpha,r,z_{las},t_{las})$ were determined by solving the system of equations (2), (3)

$$\left(\frac{\partial}{\partial z_{las}} + K_r + \frac{1}{C}\frac{\partial}{\partial t_{las}} - n_{C_0}(\alpha,r,z_{las},t_{las})\sigma_{C-A}\right) \times F(\alpha,r,z_{las},t_{las}) = 0, \quad (2)$$

$$\left(\frac{\partial}{\partial t_{las}} + \sigma_{C-A}F(\alpha,r,z_{las},t_{las})\right)n_{C_0}(\alpha,r,z_{las},t_{las}) = 0. \quad (3)$$

Here, K_r is the coefficient of attenuation of the laser beam fluence caused by the beam divergence [18] and σ_{C-A} is the stimulated-emission cross section for the C–A transition. System of equations (2), (3) was solved by the Runge–Kutta method with a constant step: $h_z = h_t c$ [19]. The step h_z was chosen so as to make the variation in fluence F within this step be no larger than 5% of the maximum F value at this instant. In the opposite case, the step h_z was reduced, and the $n_{C_0}(\alpha,r,z_{las},t_{las})$ and $F(\alpha,r,z_{las},t_{las})$ values were recalculated for the new grid. The calculation accuracy was controlled proceeding from the difference between the total number of laser radiation photons in the beam and the total number of XeF(C) molecules destroyed by induced radiation. The error of the calculations did not exceed 1%.

The model was tested on mixtures of different gases at different pump energies: E_{VUV} = 220 J [20,21], 260 J [21] and 270 J [13]. In all cases, the calculated and measured dependences of the gain on the distance to windows (*1*) (Fig. 1) were in good agreement. The amplification of a test signal in a XeF(C–A) amplifier with mirror system A was investigated in [20]. The amplified signal was cw radiation of a Sapphire 488 HP laser with λ = 488 nm and average power of 25 mW. The gain was calculated as the ratio of the output power for pumped amplifier to the output power in the absence of pumping. All simulation results and experimental data obtained at different pressures, gas mixture compositions, and VUV pump energies, are in good agreement.

In this study, we investigated (using computational methods) the change in the output energy of the XeF(C–A) amplifier for different configurations of mirror systems and pump energies varied from 270 to 400 J. The computation was carried out for a gas mixture $N_2:XeF_2$ = 380:0.2 Torr. The input pulse FWHM was 50 ps. The time dependence of the pump power, $P_{VUV}(t)$, was determined from the current and voltage oscillograms of the vacuum diode and normalised to pump energy [20,21]. The leading edge width of $P_{VUV}(t)$ was 100 ns, and the pump pulse width at the base level was 330 ns. The laser beam introduction time into the amplifier, t_{in}, was chosen so as to provide a maximum laser beam energy at the amplifier output. For scheme A, t_{in} was 80 ns (in agreement with the data of [13]). For scheme B, t_{in} increased to 100 ns.

3. Simulation results and discussion

The influence of the energy E_{in} of the input pulse with a Gaussian fluence on the output energy E_{out} was investigated in [13]. Calculations were performed for mirror scheme A at E_{VUV} = 270 J. It was shown that the amplifier switches to the saturation regime at E_{in} > 2 mJ. At this instant, the relative burnup $\Delta(XeF(C_0))$ of $XeF(C_0)$ molecules on the beam axis (R = 0) and on the lateral boundary ($R = R_{max}$) exceeds 90%. The input beam energy at which this occurs will be referred to as the gain saturation energy (E_{ins}). To determine the dependence of E_{ins} on the pump energy E_{VUV}, the influence of the input pulse energy on the output energy was numerically analysed for schemes A and B. Figure 3 shows the calculated dependences $E_{out}(E_{in})$ at E_{VUV} = 270 and 400 J. The relative burnup $\Delta(XeF(C_0))$ values for the laser beam axis and lateral boundary at E_{VUV} = 270 and 400 J, as well as the input pulse energy E_{in} at which these values were obtained, are listed in Table 1.

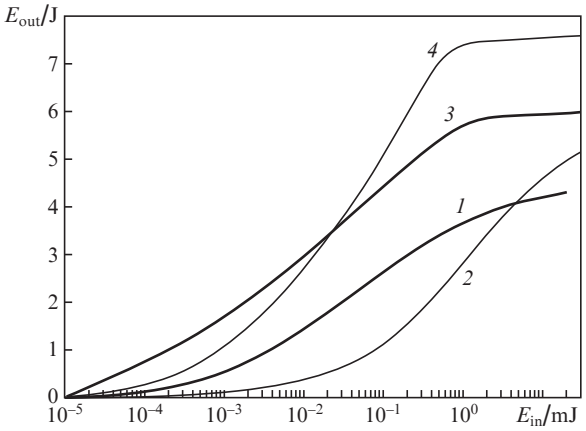

Figure 3. Dependences of E_{out} on E_{in} at E_{VUV} = (*1*,*2*) 270 and (*3*,*4*) 400 J for schemes (*1*,*3*) A and (*2*,*4*) B; R_0 = 0.5 cm.

Table 1. Relative burnup of $XeF(C_0)$ molecules.

Mirror scheme	E_{VUV}/J	E_{in}/mJ	$\Delta(XeF(C_0))$ (%)	
			R = 0	$R = R_{max}$
A	270	2.0	98.6	91.0
	400	2.0	99.0	98.0
B	270	30.0	92.0	91.0
	400	2.0	99.0	98.0

The $\Delta(XeF(C_0))$ value was calculated from the difference in the $XeF(C_0)$ concentrations at the instants of laser beam arrival at the point under consideration and the beam emergence from this point. The data are presented for the region of maximum burnup. For schemes A and B, these are the active region boundaries before mirror 31 and output window 27, respectively (see Figs 1 and 2).

For scheme A, at E_{in} > 2 mJ, a relative burnup exceeding 90% was observed both at the beam centre and on the beam lateral boundary in the entire range of variation in E_{VUV}.

In the case of scheme B, at E_{VUV} = 400 J and E_{in} = 2 mJ, more than 98% $XeF(C_0)$ molecules burn up at the beam centre and on the lateral boundary. With a decrease in E_{VUV}, the E_{ins} value increases and reaches 30 mJ at E_{VUV} = 270 J. The calculated dependence of E_{ins} on E_{VUV} is shown in Fig. 4.

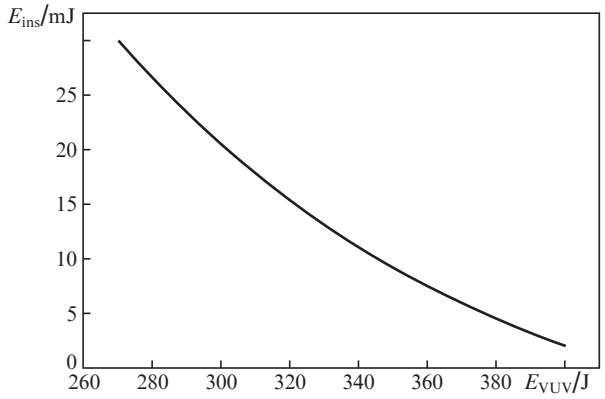

Figure 4. Dependence of E_{ins} on E_{VUV} for scheme B.

Below, in all calculations for scheme B, the input beam energy was chosen from the condition $E_{in} = E_{ins}(E_{VUV})$. In the case of scheme A, the energy $E_{in} = 2$ mJ was used for all E_{VUV} values.

The dependences of E_{out} on energy E_{VUV} for schemes A and B are shown in Fig 5. An increase in E_{VUV} leads to a rise in E_{out} for both schemes. The output energies for scheme B were found to exceed those for scheme A in the entire range of variation in E_{VUV}. At $E_{VUV} = 270$ J, the output energy for scheme A amounts to 3.36 J, whereas for scheme B it increases to 4.8 J (in this case, $E_{in} = 30$ mJ). The maximum energies at the amplifier output were obtained at $E_{VUV} = 400$ J: 5.8 and 7.58 J for schemes A and B, respectively.

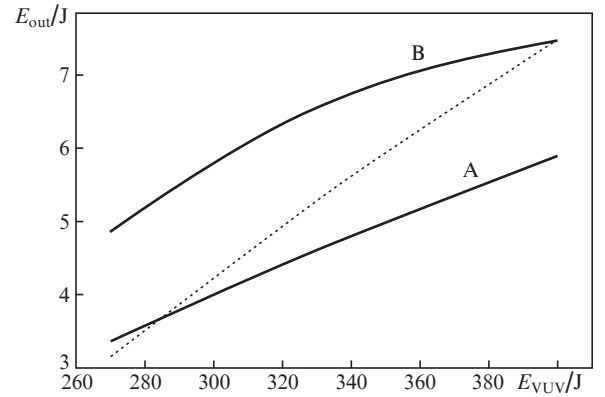

Figure 5. Dependences of E_{out} on E_{VUV} for schemes A ($E_{in} = 2$ mJ) and B [$E_{in} = E_{ins}(E_{VUV})$]; the dotted line is the dependence for scheme B at $E_{in} = 2$ mJ.

The laser beam path length S_{las} in the amplifier is 44.88 and 36.7 m for schemes A and B, respectively; therefore, at a low input radiation energy and pump energy $E_{VUV} = 270$ J, scheme B is less efficient. The dependence of E_{out} on E_{VUV}, obtained for scheme B at constant input pulse energy ($E_{in} = 2$ mJ), is shown in Fig. 5 by a dotted line. At $E_{VUV} = 270$ J, the output energy is 3.12 J. The relative burnup of $XeF(C_0)$ molecules in the region of output window at the centre of the beam and on its boundary amounts to 83% and 72%, respectively.

When analysing the possibilities of implementing experimentally the above-considered amplification regimes, an important factor is the maximum laser beam intensity I_{max} obtained in the amplifier. As calculations showed, when E_{VUV} increases in the gain saturation regime, I_{max} grows more rapidly than the laser energy. This is especially characteristic of scheme A. The reason is the decrease in the pulse width T_{fw}. Figure 6 shows the calculated dependences of the output pulse width on the pump energy for schemes A and B. According to the results of numerical simulation at $E_{VUV} = 270$ J, $T_{fw} = 18.5$ for scheme A and 20 ps for scheme B. An increase in E_{VUV} to 400 J reduces T_{fw} to 1.8 and 9.7 ps for schemes A and B, respectively.

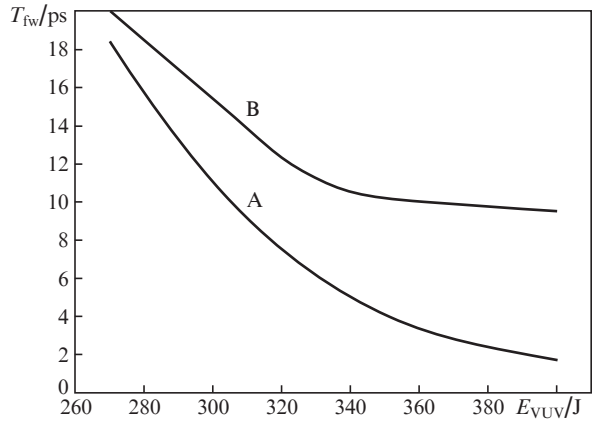

Figure 6. Dependences of T_{fw} on E_{VUV} for schemes A and B; $E_{in} = E_{ins}(E_{VUV})$.

The calculations of [13, 22] for scheme A yielded a decrease in the output pulse width from 50 ps at the amplifier input to 18 ps at the amplifier output, with good agreement between the experimental and simulated values of the output energy (3.2 and 3.8 J, respectively). The adaptive grid method used in this study improved the calculation accuracy. Energy of 3.3 J was obtained for the experimental conditions of [13] (see Fig. 5); this value is well consistent with the experimental data.

A decrease in the pulse width with an increase in the output laser energy in the case of scheme A leads to a more rapid rise in intensity than for scheme B. The dependences $I_{max}(E_{VUV})$ calculated for schemes A and B are shown in Fig. 7.

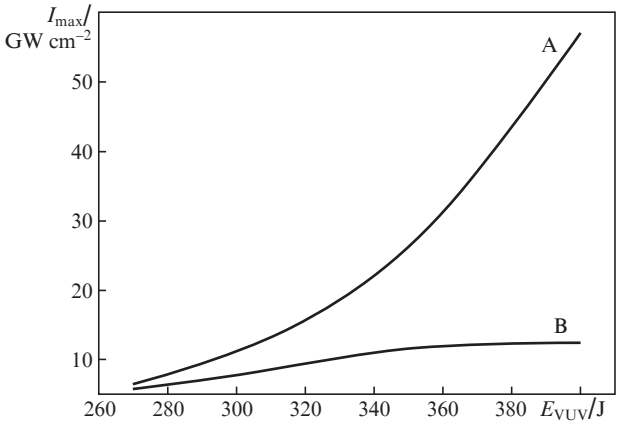

Figure 7. Dependences of I_{max} on E_{VUV} for schemes A ($E_{in} = 2$ mJ) and B [$E_{in} = E_{ins}(E_{VUV})$].

When using scheme A, the maximum beam intensity increases from 6.33 GW cm^{-2} at E_{VUV} = 270 J to 57.0 GW cm^{-2} at E_{VUV} = 400 J, which is close to the I_{max} value obtained in [11]. However, the output energy E_{out} = 5.8 J is higher by a factor of 1.88 in our case.

The maximum values of I_{max} obtained within scheme B were much smaller. According to the calculation data, an increase in E_{VUV} to 400 J increases I_{max} from 2.34 to 14.8 GW cm^{-2}, a value differing little from the calculation result (12 GW cm^{-2}) obtained in [13] for scheme A. Hence, one would expect this amplification regime to be experimentally implemented.

The dependence of the internal efficiency η_{in} of conversion of the pump energy absorbed in the amplifier gas mixture into the laser energy on E_{VUV} is shown in Fig. 8. In the saturation regime, the internal efficiency for scheme B increases from 2.8% at E_{VUV} = 270 J to 3.2% at E_{VUV} = 350 J. When using scheme A, the internal efficiency does not exceed 2.41%.

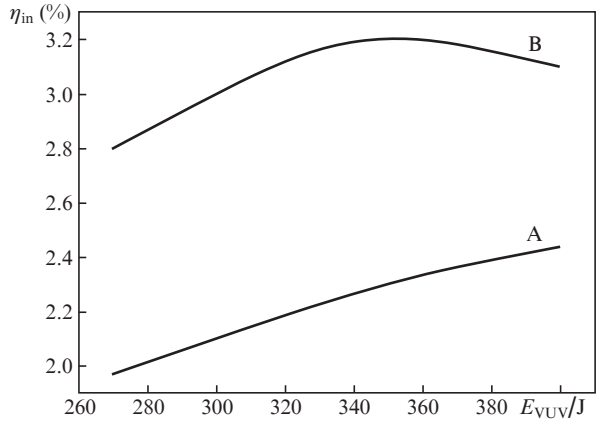

Figure 8. Dependences of the conversion efficiency of the pump energy absorbed in the amplifier active medium into the laser energy for schemes A (E_{in} = 2 mJ) and B [$E_{in} = E_{ins}(E_{VUV})$].

Some part of the pump radiation propagating in the laser cell is absorbed by opaque regions (2) (see Figs 1 and 2) and returns to windows (1). An increase in E_{VUV} from 270 to 400 J makes the pump energy loss in these processes vary within 36.5%–40%, reaching a minimum at $E_{VUV} \approx$ 300 J. With allowance for this energy loss, the efficiency with respect to E_{VUV} changes within 1.22% – 1.5% for scheme A and within 1.77% – 1.87% for scheme B.

4. Conclusions

The amplification of a 50-ps laser pulse in the XeF(C–A) amplifier of the THL-100 laser system at an increase in the pump energy from 270 to 400 J was investigated by numerical simulation. Two schemes of amplifier mirrors were considered. Scheme A (which is currently used in practice) implies 33 passes of the amplified pulse through the active medium. The input beam divergence angle in this scheme is 0.95 mrad. In scheme B, the number of passes through the active medium is reduced to 27, and the beam divergence angle is increased to 1.78 mrad.

Dependences of the output laser pulse energy on the input pulse energy were obtained for both schemes at VUV pump energies of 270 J (experiment) and 400 J (calculation). It was shown that amplifier saturation for scheme A occurs at $E_{ins} \approx$ 2 mJ in this range of variation in E_{VUV}. Using scheme B, one can reduce the E_{ins} value from 30 mJ at E_{VUV} = 270 J to 2 mJ at E_{VUV} = 400 J.

It was shown that, with an increase in the pump energy to 400 J in the amplifier saturation regime, scheme A makes it possible to increase the laser pulse energy at the amplifier output to 5.3 J at a maximum laser radiation intensity of 57 GW cm^{-2}.

It was also shown that, at the currently used amplifier pump energy (270 J), the application of mirror scheme B makes it possible to increase (in comparison with scheme A) the output energy to 4.8 J at input energy of 30 mJ. According to the simulation data, an increase in the pump energy to 400 J makes it possible to increase the output energy to 7.5 J at a maximum radiation intensity not higher than 14.8 GW cm^{-2}.

The maximum conversion efficiency of the pump energy absorbed in the amplifier laser cell into the laser energy is 2.41% and 3.2% for schemes A and B, respectively.

Acknowledgements. This work was supported by the Russian Foundation for Basic Research (Grant No. 16-08-00204).

References

1. Strickland D., Mourou G. *Opt. Commun.*, **56**, 219 (1985).
2. Ozaki T., Keiffer J.C., Toth R., Fourmaux S., Bandulet H. *Laser Part. Beams*, **24**, 101 (2005).
3. Basov N.G., Zuev V.S., Mikheev L.D., Stavrovskii D.B., Yalovoi V.I. *Sov. J. Quantum Electron.*, **7**, 1404 (1977) [*Kvantovaya Elektron.*, **4**, 2453 (1977)].
4. Mikheev L.D. *Laser Part. Beams*, **10**, 473 (1992).
5. Basov N.G., Zuev V.S., Kanaev A.V., Mikheev L.D., Stavrovskii D.B. *Sov. J. Quantum Electron.*, **9**, 629 (1979) [*Kvantovaya Elektron.*, **6**, 1074 (1979)].
6. Tcheremiskine V.I., Sentis M.L., Mikheev L.D. *Appl. Phys. Lett.*, **81**, 403 (2002).
7. Malinovskii G.Ya., Mamaev S.B., Mikheev L.D., Moskalev T.Yu., Sentis M.L., Cheremiskin V.I., Yalovoi V.I. *Quantum Electron.*, **31**, 617 (2001) [*Kvantovaya Elektron.*, **31**, 617 (2001)].
8. Tcheremiskine V., Uteza O., Mislavskii V., Sentis M., Mikheev L. *Proc. SPIE*, **6346**, 634613 (2007).
9. Alekseev S.V., Aristov A.I., Grudtsyn Ya.V., Ivanov N.G., Koval'chuk B.M., Losev V.F., Mamaev S.B., Mesyats G.A., Mikheev L.D., Panchenko Yu.N., Polivin A.V., Stepanov S.G., Ratakhin N.A., Yalovoi V.I., Yastremskii A.G. *Quantum Electron.*, **43**, 190 (2013) [*Kvantovaya Elektron.*, **43**, 190 (2013)].
10. Alekseev S.V., Aristov A.I., Ivanov N.G., Kovalchuk B.M., Losev V.F., Mesyats G.A., Mikheev L.D., Panchenko Yu.N., Ratakhin N.A. *Laser Part. Beams*, **31**, 17 (2013).
11. Yastremskii A.G., Ivanov M.V., Ivanov N.G., Losev V.F. *Opt. Atmos. Okeana*, **29**, 121 (2016).
12. Alekseev S.V., Ivanov N.G., Ivanov M.V., Losev V.F., Mesyats G.A., Mikheev L.D., Panchenko Yu.N., Ratakhin N.A., Yastremskii A.G. *Izv. Vyssh. Uchebn. Zaved., Ser. Fiz.*, **60** (8), 75 (2017).
13. Yastremskii A.G., Ivanov N.G., Losev V.F. *Quantum Electron.*, **46**, 982 (2016) [*Kvantovaya Elektron.*, **46**, 982 (2016)].
14. Losev V.F., Alekseev S.V., Ivanov M.V., Ivanov N.G., Mesyats G.A., Mikheev L.D., Panchenko Yu.N., Ratakhin N.A., Yastremsky A.G. *Proc. SPIE*, **10254**, 1025415 (2017).
15. Alekseev S.V., Ivanov N.G., Ivanov M.V., Losev V.F., Mesyats G.A., Mikheev L.D., Panchenko Yu.N., Ratakhin N.A., Yastremskii A.G. *Quantum Electron.*, **47**, 184 (2017) [*Kvantovaya Elektron.*, **47**, 184 (2017)].
16. Ivanov N.G., Losev V.F., Panchenko Yu.N., Yastremskii A.G. *Opt. Atmos. Okeana*, **27**, 1 (2014).
17. Fletcher C.A.J. *Computational Techniques for Fluid Dynamics* (Springer, Heidelberg, 1991; Moscow: Mir, 1991).
18. Kuznetsova T.I., Mikheev L.D. *Quantum Electron.*, **38**, 969 (2008) [*Kvantovaya Elektron.*, **38**, 969 (2008)].

19. Fleck J.A. Jr. *Phys. Rev. B*, **1**, 84 (1970).
20. Alekseev S.V., Ivanov N.G., Losev V.F., Panchenko Yu.N., Yastremskii A.G. *Opt. Atmos. Okeana*, **26**, 863 (2013).
21. Losev V., Alekseev S., Ivanov N., Kovalchuk B., Mikheev L., Mesyats G., Panchenko Yu., Puchikin A., Ratakhin N., Yastremsky A. *Proc. SPIE*, **7993**, 799317 (2011).
22. Ivanov N.G., Ivanov M.V., Losev V.F., Yastremskii A.G. *Izv. Vyssh. Uchebn. Zaved., Ser. Fiz*., **59** (7), 65 (2016).